Abdominal Radiology

Published online: 11 October 2018

Abdom Radiol (2019) 44:1430–1452
https://doi.org/10.1007/s00261-018-1789-4

Uncommon malignant renal tumors and atypical presentation of common ones: a guide for radiologists

Benjamin Laguna,[1] Antonio C. Westphalen,[1,2] C. T. Guimarães,[2] Zhen Whang,[1,2] Jeff Simko,[3] and Ronald Zagoria[1,2]

[1]Department of Diagnostic Radiology, University of California, San Francisco, 505 Parnassus, San Francisco, CA 94122, USA
[2]Department of Abdominal Imaging, University of California, San Francisco, 505 Parnassus, San Francisco, CA 94122, USA
[3]Department of Anatomic Pathology, Radiation Oncology, Urology, University of California, San Francisco, 505 Parnassus, San Francisco, CA 94122, USA

Abstract

Objective: While the typical imaging features of the more common RCC subtypes have previously been described, they can at times have unusual, but distinguishing features. Rarer renal tumors span a broad range of imaging features, but they may also have characteristic presentations. We review the key imaging features of atypical presentations of malignant renal tumors and uncommon malignant renal tumors.
Conclusion: Renal tumors have many different presentation patterns, but knowledge of the distinguishing MR and CT features can help identify both atypical presentation of common malignancies and uncommon renal tumors.

Key words: CT—MRI—RCC—Kidney—Neoplasm

Approximately 90% of renal malignancies are renal cell carcinomas (RCC), and 85% of these are clear cell (ccRCC), papillary (pRCC), or chromophobe (chRCC) subtypes [1]. Although the typical imaging appearance of these more common RCC subtypes has been extensively described, at times they can have unusual features. The remaining 15% comprises rarer renal tumors with a broad range of possible imaging presentations. However, despite their rarity, many have characteristic presentations. Knowledge of the atypical imaging features of common renal tumors and the typical imaging features of uncommon renal tumors is important not only for prognostic purposes and guiding management, but also in cases where tissue sampling cannot be obtained (e.g., patient refusal or high-risk patients). Correctly characterizing a renal lesion may eliminate the need for underlying biopsy, or suggest alternative management, such as renal ablation or observation. Furthermore, knowledge of key clinical information in conjunction with imaging features, including past medical history and patient age, is often critical in narrowing the differential diagnosis.

Renal tumors are a heterogeneous group, and their classification is summarized in the 2016 World Health Organization (WHO) scheme [2]. This article will follow a similar organization and nomenclature to summarize their imaging characteristics (Tables 1, 2).

Common renal malignancies

Renal cell carcinoma encompasses approximately 90% of all renal malignancies [2]. Exposure to carcinogens, including tobacco smoking, arsenic, and other environmental exposures increases the risk of RCC. Solid enhancing renal masses on imaging are suspicious for RCC. Additional imaging features can help to further differentiate among RCC subtypes, with the most common ones including ccRCC, pRCC, and chRCC. Furthermore, the Bosniak classification of predominantly cystic renal lesions helps radiologists to identify lesions that are cystic RCCs.

Clear cell RCC

Clear cell RCC is the most common subtype of RCC, accounting for nearly 75% of RCCs, an approximately 6:1 male-to-female predominance, and carries a prog-

Correspondence to: Benjamin Laguna; *email:* Benjamin.Laguna@ucsf.edu

Table 1. Common malignant renal tumors

Tumor type	Imaging features	Prognosis	Associations
ccRCC	Heterogeneous T2 hyperintense Intense enhancement Intracellular fat Increased relative enhancement during corticomedullary phase Increased ADC values	Most aggressive	VHL syndrome
pRCC Type 1	Homogeneous T2 hypointense Minimal enhancement Hemosiderin Cyst with papillary projections Macroscopic fat within a mass that cystic/contains calcifications	Better prognosis	Hereditary papillary RCC syndrome
pRCC Type 2	Indistinct margins Heterogeneity	Worse prognosis	Hereditary leiomyomatosis RCC syndrome
chRCC	Well-circumscribed Intermediate peripheral enhancement Central scar (40%) Overlapping features with oncocytoma	Least aggressive	Birt–Hogg–Dubé syndrome

ccRCC clear cell renal cell carcinoma, *pRCC* papillary renal cell carcinoma, *chRCC* chromophobe renal cell carcinoma

Table 2. Uncommon malignant renal tumors

Tumor type	Imaging characteristics	Prognosis/clinical features
Multilocular cystic renal neoplasm	Well circumscribed, cysts with serous of hemorrhagic fluid, and pseudocapsule Classified using Bosniak IIF to IV	Excellent prognosis Indistinct from cystic nephroma
Collecting duct carcinoma (Bellini)	Large, heterogeneous, infiltrative, often with cystic components. Hypovascular and low T2 signal	Highly aggressive. Triad of abdominal pain, flank mass, and hematuria
Renal medullary carcinoma	Large and infiltrative, often centered in the medulla. Can contain hemorrhage, necrosis, and/or calcifications. Low T2 signal	Sickle cell trait Poor prognosis
Neuroendocrine tumor	*Carcinoid* circumscribed, calcifications, low-level enhancement, horseshoe kidney *Neuroendocrine carcinoma* large, no necrosis, low-level enhancement, medullary	Well-differentiated vs. poorly differentiated
Nephroblastic/Wilm's tumor	*Wilm's* circumscribed, lobulated, necrosis, calcifications, and old hemorrhage *Nephrogenic rests* perilobar vs. intralobar. Peripheral, round low-level enhancement	Most common renal neoplasms in children
Mesenchymal tumors	Large, heterogeneous, perinephric extension Components corresponding to precursor cells	Highly aggressive
RCC Xp11.2 translocation/TFE3 gene fusion (subtype of RCC)	Medullary, hyperdense, capsule sign, lymph nodes, low/heterogenous T2 signal	Aggressive, < 45 years female predilection
hematopoietic/lymphoid	*Lymphoma* 5 patterns (diffuse infiltration, retroperitoneal, perirenal solitary, or multiple masses) *Leukemia* nodular infiltration, nephromegaly	Renal involvement seen in advanced-stage
Metastases	Bilateral, multifocal, or infiltrative	Late-stage disease, often indicating multisystemic disease Commonly from bronchogenic carcinoma, gastrointestinal and breast cancer

RCC renal cell carcinoma

nosis of 44–69% survival at 5 years [3, 4]. These are pathologically characterized by the presence of malignant cells with clear or eosinophilic cytoplasm within a vascular network [5]. Macroscopically, clear cell RCCs are typically well-demarcated cortically based solitary lesions, often containing a pseudocapsule. These masses frequently contain cystic areas, necrosis, hemorrhage, and/or calcifications. When ccRCCs extend beyond the kidney, they may invade the Gerota's fascia, grow into the renal vein and the vena cava, and metastasize hematogenously. Spread beyond the renal capsule or renal vein, extension is present in up to 45% of ccRCC cases at presentation, and accounts for 94% of metastatic RCC [3, 6].

On imaging, ccRCCs (Figs. 1, 2, 3, 4) classically present as solid masses with intense heterogeneous contrast-enhancement on both CT and MRI [3]. On MRI, these tumors typically show higher T2 signal intensity

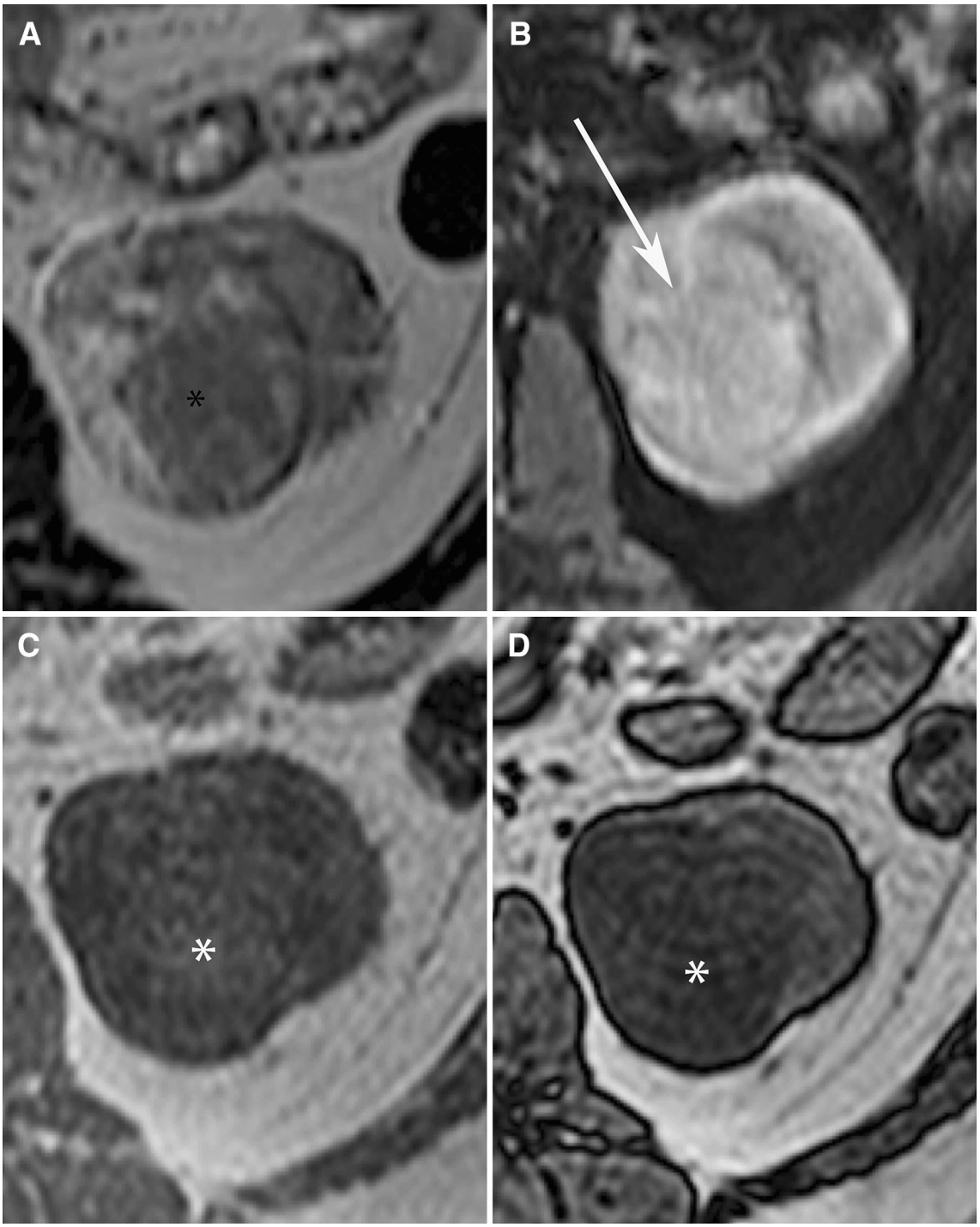

Fig. 1. Typical features of clear cell RCC. **A** Axial T2W shows heterogeneous kidney lesion (black asterisk); **B** intense enhancement on axial post-contrast T1W fat-suppressed (white arrow); **C** T1W in phase (white asterisk) and **D** T1W out of phase show drop signal (white asterisk) corresponding to intracellular fat.

than the normal parenchyma, and are hypo or isointense on T1-weighted (T1W) images [7]. Of note, the presence of intracellular lipid, diagnosed when there is a relative drop of signal on opposed-phase gradient echo images compared to in-phase images, is highly suggestive of a ccRCC [3]. Other advanced imaging techniques have also been shown to be helpful differentiating ccRCC from other subtypes. For example, ccRCC has been shown to have increased relative enhancement within the corticomedullary phase on multiphasic MRI and CT compared to other RCC subtypes [8, 9]. Additionally, DWI/ADC has been helpful in differentiating ccRCC, with

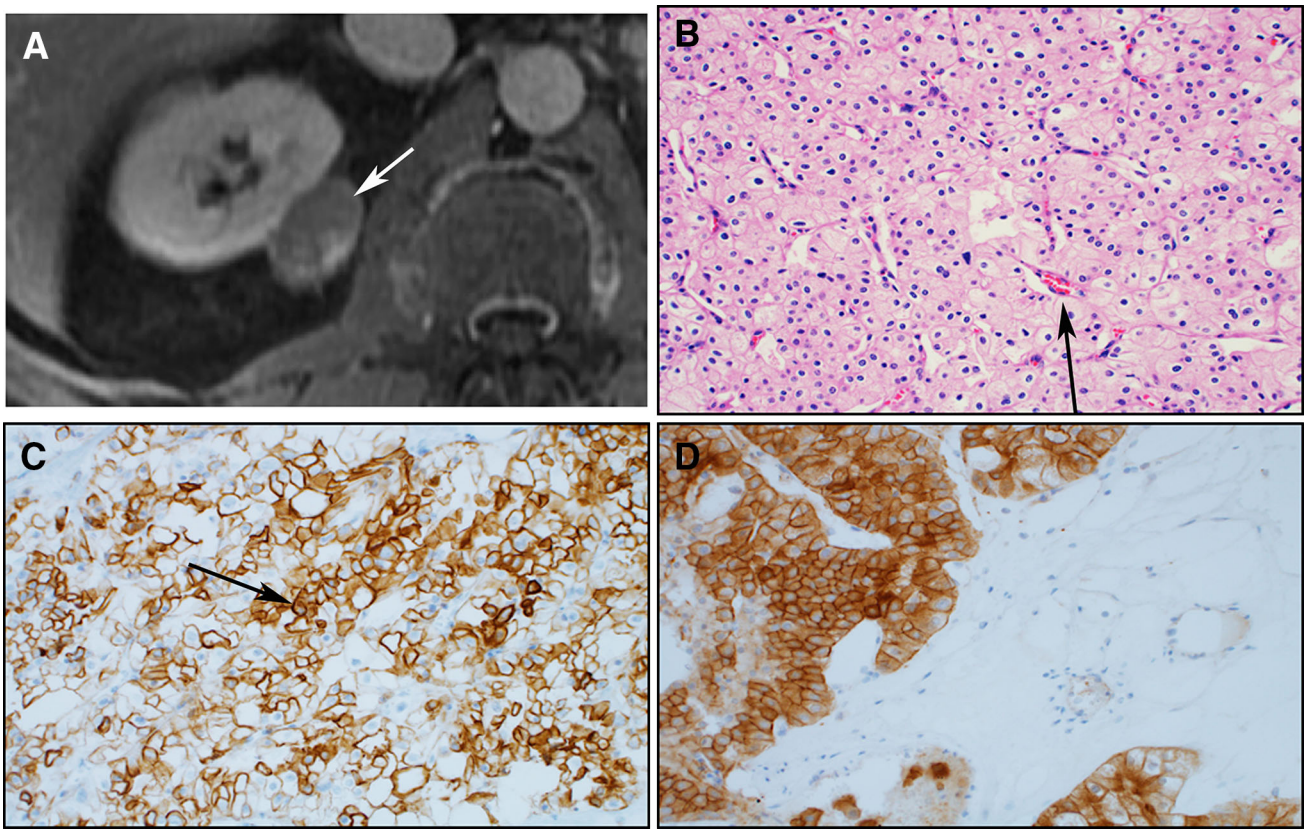

Fig. 2. Clear cell RCC example. **A** Axial post-contrast T1W shows well-circumscribed renal mass, enhancing less than cortex (white arrow); **B** Photomicrograph (original magnification, × 200; H–E stain) shows small vessels (black arrow) apart and big nucleus sometimes binucleated; **C** Photomicrograph (original magnification, × 200; CK7 immunostain) diffusely positive on cCCR (black arrow), differentiating from oncocytomas, **D** Photomicrograph (original magnification, × 200; CD117 immunostain) positive corroborating cCCR.

ccRCC demonstrating increased ADC values when compared to other RCC subtypes [10, 11].

Atypical presentation of clear cell RCC

Clear cell RCC develops in 25–45% of patients with Von Hippel–Lindau (VHL) syndrome [12]. In these patients, ccRCC are often multiple, bilateral solid masses, or complex cystic tumors [13, 14]. These patients also commonly have pancreatic and renal cysts, pheochromocytomas, and central nervous system tumors [15] (Fig. 5).

Papillary RCC

Papillary RCC's (Figs. 6, 7, 8, 9, 10) comprise about 10% of RCC's, with an approximate 3:1 male-to-female ratio, and a 5-year survival rate of 82–92% [3, 4]. pRCCs are more often bilateral and multifocal than other RCCs subtypes. This tumor subtype is histologically characterized by a papillary or tubulopapillary architecture [7]. pRCCs are further classified into Type 1, Type 2, and mixed tumors [16]. Type 1 tumors have papillae covered by small cells with scant cytoplasm, arranged in a single layer, and are more often multifocal. Type 2 tumors are far less common and have a higher nuclear grade, with eosinophilic cytoplasm and pseudostratified nuclei on papillary cores. Macroscopically, pRCCs are characterized by areas of hemorrhage, necrosis, and cystic degeneration. These tumors are prone to bleeding and can lead to spontaneous perirenal hemorrhage [17]. Because of this propensity to bleed, pRCCs more commonly contain hemosiderin than other tumors, and this imaging finding aids in their diagnosis with MRI [18].

On imaging, pRCCs usually demonstrate homogenous and low-level enhancement pattern, with a lower tumor-to-normal parenchyma enhancement ratio, when compared to ccRCCs [3, 7, 9]. Additionally, tumor ADC values tend to be between those found in ccRCC and chromophobe RCC [19]. The presence of hemosiderin is confirmed by a relative drop of signal intensity on in-phase compared to opposed-phase gradient echo images. Type 1 tumors characteristically present as T2-weighted (T2W) hypointense, hypoenhancing solid masses, and/or as a cystic mass with enhancing mural solid papillary projections. Type 2 tumors are much less common, larger masses with indistinct margins and heterogeneous T2W

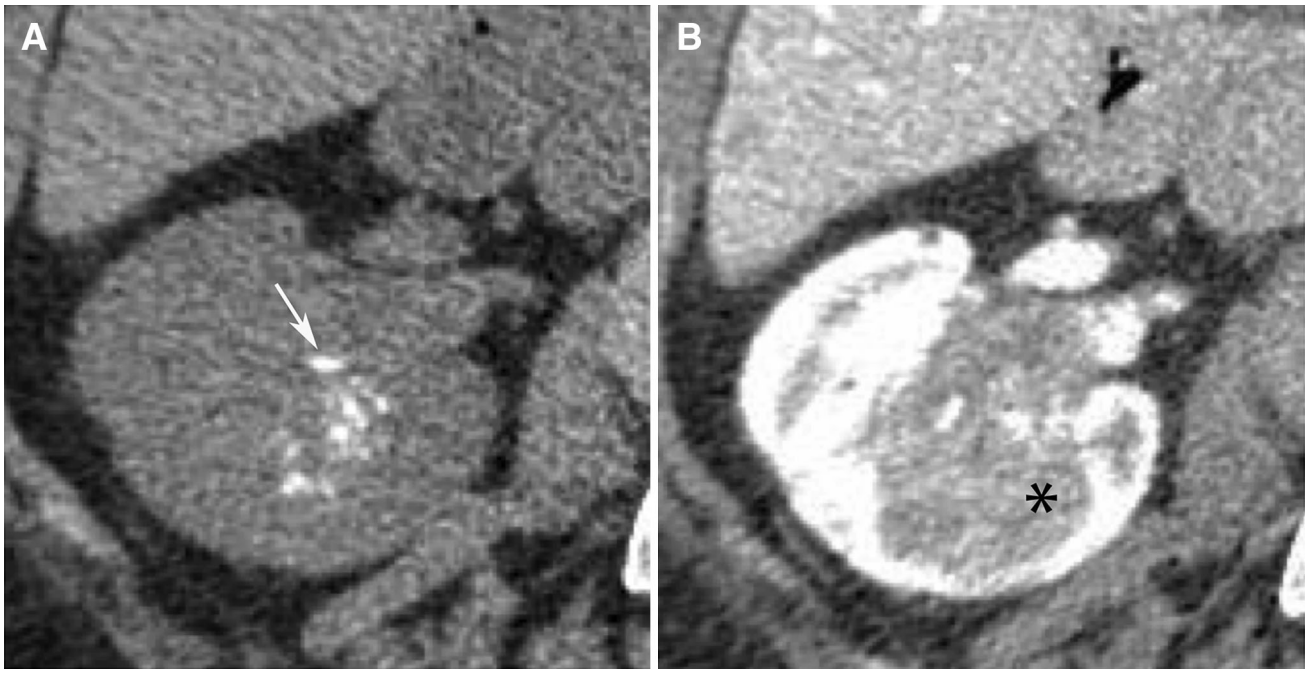

Fig. 3. Proven clear cell RCC. **A** Axial non-enhanced CT confirms the calcifications (white arrow) and **B** Axial CECT shows the associated renal mass (black asterisk).

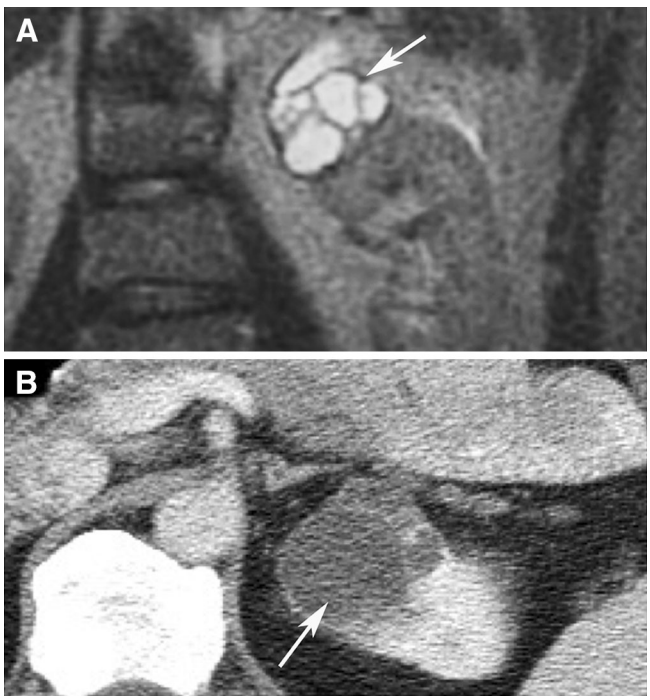

Fig. 4. Confirmed clear cell RCC. **A** Coronal T2W MR image demonstrating T2 intense mass (white arrow) and **B** Axial CECT showing complex cystic mass (white arrow).

signal and enhancement. However, imaging features overlap between the two subtypes. Patients with Type 1 tumors tend to have better survival rates.

Atypical presentation of papillary RCC

Papillary RCC can have an atypical presentation in patients with hereditary papillary renal cell carcinoma (HPRC), caused by pathogenic variants in the MET gene, and hereditary leiomyomatosis and renal cell cancer (HLRCC), caused by pathogenic variants in the FH gene [20–22]. HPRC is an autosomal dominant disease with approximate 100% penetrance. Patients present with early onset multifocal, bilateral type 1 papillary tumors. HLRCC is also an autosomal dominant disease with high penetrance, but not all patients develop RCCs. Patients typically demonstrate cutaneous and uterine leiomyomas, with a prevalence of RCCs estimated in approximately 30%. These are type 2 pRCCs, usually high grade and solitary. Rarely, pRCCs will contain foci of macroscopic fat, which can mimic angiomyolipoma [23, 24]. However, the diagnosis of pRCC should be presumed when the mass also is cystic and/or contains calcifications. The fat is thought to be from necrosis of cholesterol laden macrophages in the pRCC.

Chromophobe RCC

Chromophobe RCCs (Figs. 11, 12) comprise approximately 5% of renal epithelial tumors and are characterized histologically by large pale cells with prominent cell membranes [25]. It preferentially affects adults, with similar incidences in men and women, and a 5-year survival rate of 44–69% [3]. These tumors are the least aggressive of the RCC subtypes. chRCC are usually

Fig. 5. von Hippel–Lindau syndrome. **A** Axial fat-suppressed T2W shows multiple pancreatic cysts (white arrow); **B** Axial post-contrast T1W fat-suppressed image shows solid mass on the right kidney (white arrow); and **C** Axial post-contrast T1W fat-suppressed imaged shows complex cyst on the left kidney corresponding to clear cell RCCs (white arrow).

homogeneous, well-circumscribed masses with lobulated borders, without local extension or vascular invasion. Importantly, these lesions have overlapping imaging and histologic features with oncocytomas and up to 17% of oncocytomas are hybrid oncocytic tumors containing areas of chRCC [26, 27].

On imaging, chromophobe RCC is typically a solid, well-circumscribed renal mass, with an enhancement pattern that is predominantly peripheral and more intense than that seen with pRCC, though less than ccRCC. Tumors with heterogeneous enhancement tend to have more aggressive behavior [25]. A central scar can be seen in chromophobe RCC, though it is not specific and can be associated with other types of RCCs and oncocytomas. Similarly, a specific pattern of enhancement called ''segmental enhancement inversion'' has

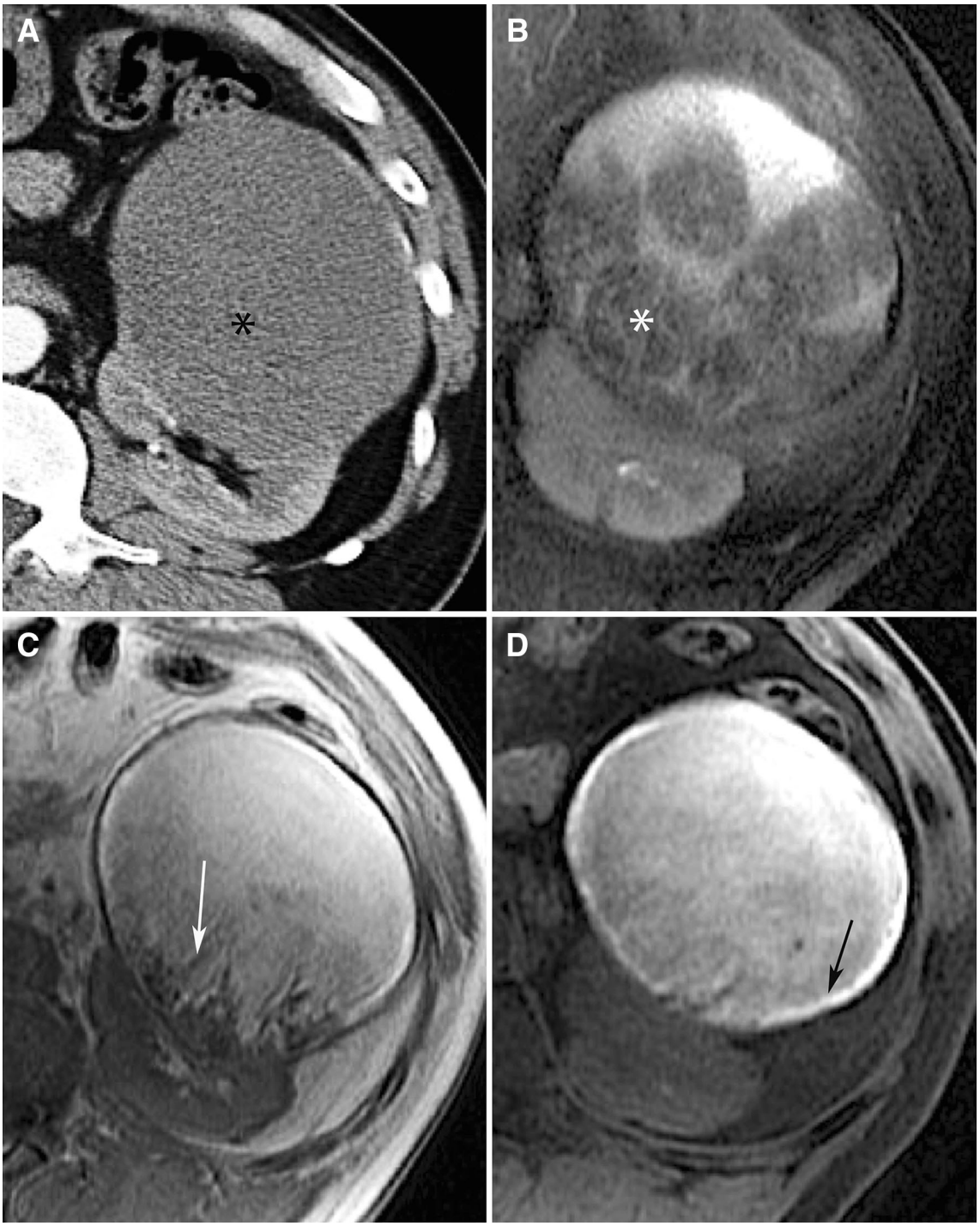

Fig. 6. Papillary RCC. **A** Axial CECT, demonstrating minimal enhancement (black asterisk); **B** axial fat-suppressed T2W, demonstrating fat signal drop out (white asterisk); **C** axial T1W demonstrating papillary projections (white arrow); **D** axial pre-contrast fat-suppressed T1W, demonstrating a T1 hyperintense rim (black arrow), characteristic of hemorrhagic content.

been described in association with oncocytomas [4, 26, 28]. This enhancement pattern is characterized by the inversion in two distinct areas of enhancement within a renal mass during the corticomedullary phase, which are subsequently inverted during the nephrographic phase. Calcifications, cystic areas, hemorrhage, or intracellular lipid are uncommon.

Fig. 7. Papillary RCC type 2. Contrast-enhanced CT images. (**A**) Coronal and (**B**) axial show heterogeneous enhancement mass with indistinct margins (white arrows).

Atypical presentation of chromophobe RCC

Birt–Hogg–Dubé syndrome is an autosomal dominant disorder caused by a variation in the folliculin gene. Patients present with cutaneous fibrofolliculomas, pulmonary cysts and spontaneous pneumothorax, and, in 15–30% of cases, renal tumors. Most RCCs are hybrid oncocytic tumors, followed by cRCC and oncocytomas. These may have be multiple and bilateral tumors [22, 29]. Other types of RCCs represent less than 5–10% of cases [22].

RCC Xp11.2 translocation and TFE3 gene fusion

These renal masses are defined by several translocations within chromosome Xp11.2, that results in fusion of the TFE3 gene [30]. Translocation lesions are a rare subtype of RCC, making up less than 3% of all RCCs, but represent 20% of renal lesions in patients less than 45 years old. Mean survival of 2 years has been reported in adults, while a mean survival rate of 6.3 years has been reported in pediatric patients [31]. They preferentially affect females and are often aggressive. On histopathology, translocation tumors are typically carcinomas with a combination of papillary RCC and clear cell RCC components [30, 32, 33]. On imaging, translocation lesions are medullary based and mildly hyperdense on non-enhanced CT images. On post-contrast imaging, they exhibit a "capsule" or a thin rim of peripheral enhancement. Additionally, because of their varied histological composition, they have heterogeneous enhancement patterns, often contain cystic or necrotic components, and sometimes calcifications [34]. On MRI, these lesions tend to have low or heterogeneous signal on T2-weighted images (Fig. 13) [31].

Uncommon renal malignancies

Multilocular cystic renal neoplasm of low malignant potential

Multilocular cystic renal neoplasm of low malignant potential constitutes less than 1% of all malignant renal tumors, and have an excellent 5-year survival rate of 100% [35]. They are more commonly seen in adult males, and have not been reported to develop metastases. These lesions are well-circumscribed masses composed of small and large cysts filled with serous or hemorrhagic fluid, and are separated from the surrounding renal parenchyma by a pseudocapsule (Fig. 14). Histopathologically, the septa that form the cysts contain large amounts of clear cells, but without aggressive growth [36]. On imaging, these are categorized as Bosniak IIF to IV, depending on the thickness of septa, presence or absence of septal or wall calcifications (seen in 20% of cases), and the presence or absence of mural nodules [36–38]. These tumors are indistinguishable from cystic nephromas.

Collecting duct carcinoma (Bellini duct carcinoma)

Collecting duct carcinomas represent less than 1% of renal neoplasms, are highly aggressive, and more commonly affect adult males [39]. The median survival rate is approximately 11 months [40]. They arise from malignant epithelial cells thought to be derived from the principal cells of the collecting duct of Bellini. Histopathologic diagnosis is challenging and often one of exclusion. This is partially due to the fact that other renal malignancies may arise centrally from cortical tissue of the columns of Bertin [41, 42]. Cells usually display high-grade features and can at times have sarcomatoid features. Patients typically present with the triad of abdominal pain, flank mass, and hematuria [43]. These tumors are usually large, centered in the medulla, infiltrative (often into the renal pelvis) (Fig. 15), heterogeneous with cystic components, hypovascular, and have low signal intensity on T2-weighted MR images [44, 45].

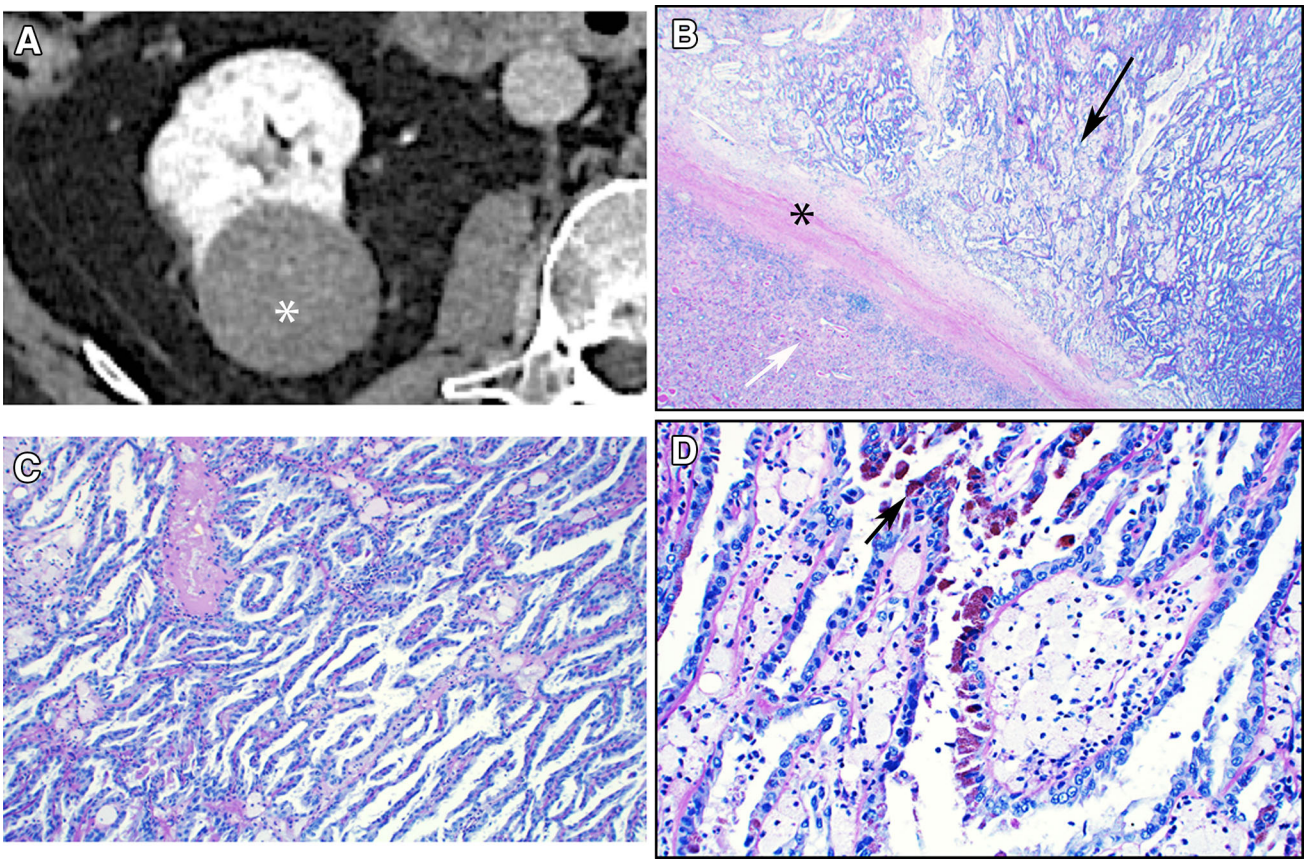

Fig. 8. Papillary RCC. (**A**) Axial CECT shows hypovascular renal mass (white asterisk); (**B**) photomicrograph (original magnification, × 20; hematoxylin–eosin stain) and (**C**) photomicrograph (original magnification, × 100; hematoxylin–eosin stain) show papillary fibrovascular cores with macrophages (black arrow), distinct fibrous capsule (black asterisk), and normal kidney (white arrow); **D** Photomicrograph (original magnification, × 200; H–E stain) shows hemosiderin common in pRCC (black arrow).

Renal medullary carcinoma

Renal medullary carcinomas are rare, but highly aggressive and rapidly growing tumors that arise from the renal medulla. They are almost exclusively seen in young male patients and have been associated with sickle cell trait, and demonstrate an overall survival rate of less than 12 months [46, 47]. They represent less than 1% of renal lesions, and over 160 cases have been reported in the literature [48]. On histopathology, renal medullary carcinomas have sheets of cells with a reticular growth pattern and adenoid cystic pathology. On imaging, renal medullary carcinomas are large and infiltrative lesions centered within the medulla (Fig. 16). Invasion of the collecting system results in caliectasis [49]. They are heterogeneous, often containing hemorrhage, necrosis, or calcifications [50]. Renal medullary carcinomas are typically hypovascular and often exhibit low T2 signal on MR imaging [50].

Renal neuroendocrine tumors

Renal neuroendocrine tumors (RNET) are rare well-differentiated tumors, usually found in adults. Carcinoid is the most common type of RNET, and patients typically present with carcinoid syndrome, in addition to the typical signs and symptoms associated with renal tumors [51]. These lesions represent less than 1% of renal tumors, and a review reported 73.1% of patients without evidence of disease after treatment, with a slight prevalence of disease among female patients [51]. They are typically well circumscribed, have minimal enhancement, can contain calcifications (25%). These tumors more commonly occur in horseshoe kidneys. A small subset of patients develop neuroendocrine carcinomas [52]. These tend to be poorly differentiated and aggressive when detected. On imaging, they are large lesions centered within the medulla, demonstrate low-level enhancement, and often lack central necrosis in spite of their size (Figs. 17, 18) [53]. Diagnostic confirmation can be performed with PET scans that target somatostatin receptors, e.g., octreotide and DOTA-TATE scans. Yet, sensitivity may be low if the tumor is poorly differentiated (Fig. 19).

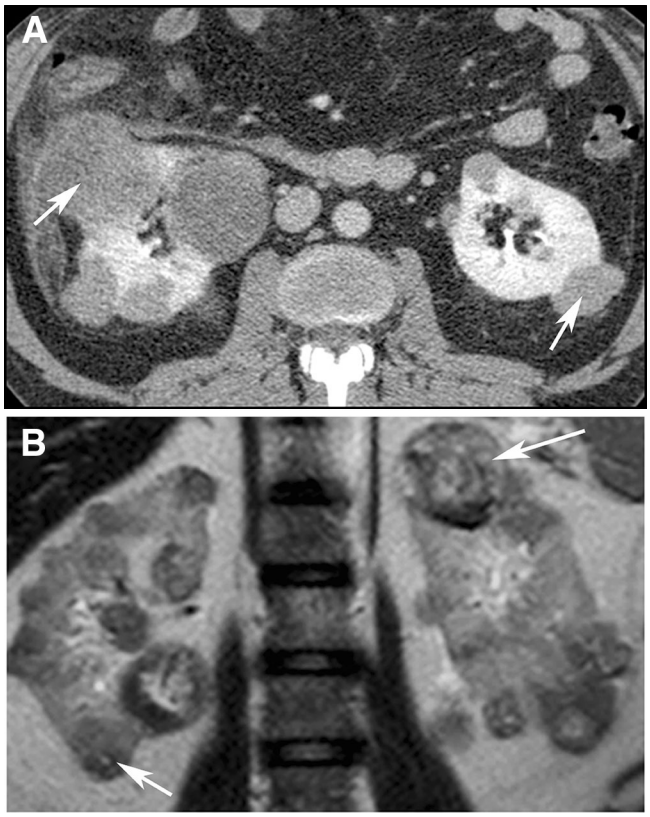

Fig. 9. Hereditary papillary RCC. **A** Axial CECT demonstrates multiple bilateral hypoenhancing masses (white arrows) and **B** coronal T2W MR images show multiple and bilateral renal masses, predominantly hypointense on T2W and with low enhancement (white arrows), related to HPRCC.

Nephroblastic lesions and Wilm's tumor

Nephrogenic rests are persistent embryonal renal tissue, found in approximately 1% of infant kidneys at biopsy [54]. Multiple areas of persistent embryonal renal tissue are known as nephroblastomatosis, a precursor to Wilms tumors [24]. Rests are classified as either perilobar or intralobar types. Perilobar rests are sharply circumscribed and located in the periphery of the renal lobe. Intralobar nephrogenic rests are centrally located, poorly circumscribed, and contain stromal elements (Fig. 20). Both types may remain dormant, regress, or undergo hyperplasia, and as many as 30–40% of cases will give rise to Wilm's tumor [54]. Hyperplastic rests are difficult to distinguish from nephroblastoma, i.e., Wilm's tumor. On imaging, nephrogenic rests are focal round masses which demonstrate poor enhancement [54]. Increase in size and heterogeneous enhancement should raise the suspicion of malignant transformation, i.e., nephroblastoma.

While nephroblastomas (Wilm's tumors) are overall rare tumors, they make up 90% of pediatric renal tumors, often presenting between 2 and 3 years, and no known gender predilection (Fig. 21) [55]. Patients typically present with abdominal masses detected by their parents. They can also present with abdominal pain, hematuria, hypertension, or abdominal crisis due to traumatic rupture of the tumor. On imaging, Wilms tumors are typically solid, well circumscribed or macrolobulated, often with necrosis, old hemorrhage, and calcifications (15%). Invasion of the renal vein and IVC is seen in 5–10% of patients. Overall survival rates can often exceed 85% [56].

Mesenchymal tumors

Mesenchymal tumors have benign and malignant subtypes, and are composed of several different cell types. These often arise from the renal capsule and are located peripheral to the kidney. Overall, malignant mesenchymal tumors are rare, representing 1–3% of all malignant renal tumors, and include leiomyosarcoma, osteosarcoma, rhabdomyosarcoma, synovial sarcoma, and malignant fibrous histiocytoma [57]. All are highly aggressive and have poor prognosis, with a 5-year survival of 29–36% [58]. On imaging, these are large heterogeneous masses associated with aggressive features, e.g., perinephric extension [58, 59]. The imaging appearance of tumor components may correspond to the precursor cells. For example, ossification may be seen in cases of renal osteosarcomas.

Hematopoietic and lymphoid tumors

In this class of malignancies, renal involvement is more common in patients with underlying lymphoma or leukemia. In patients with secondary renal lymphoma, the disease is already advanced, and is most commonly the large b cell diffuse subtype (non-Hodgkins lymphoma) [60]. Primary renal lymphoma is rare, representing less than 1% of renal tumors, with a 5-year survival rate of 40–50%, and tends to affect males more than females [61, 62]. On imaging, lymphoma has five typical patterns of presentation: it most commonly presents as multiple homogeneous infiltrating renal parenchymal masses, but can also present as a solitary mass, perirenal mass, diffuse infiltration with splenomegaly, and invasion from retroperitoneal lymph node metastasis (Figs. 22, 23) [63].

Leukemia may also involve the kidney, and some involvement is present in 90% of patients who die from leukemia. However, imaging manifestations of renal involvement is detected in less than 5% of patients. On imaging, there can be diffuse or nodular renal parenchymal infiltration, bilateral or unilateral nephromegaly from diffuse leukemic infiltration, and as

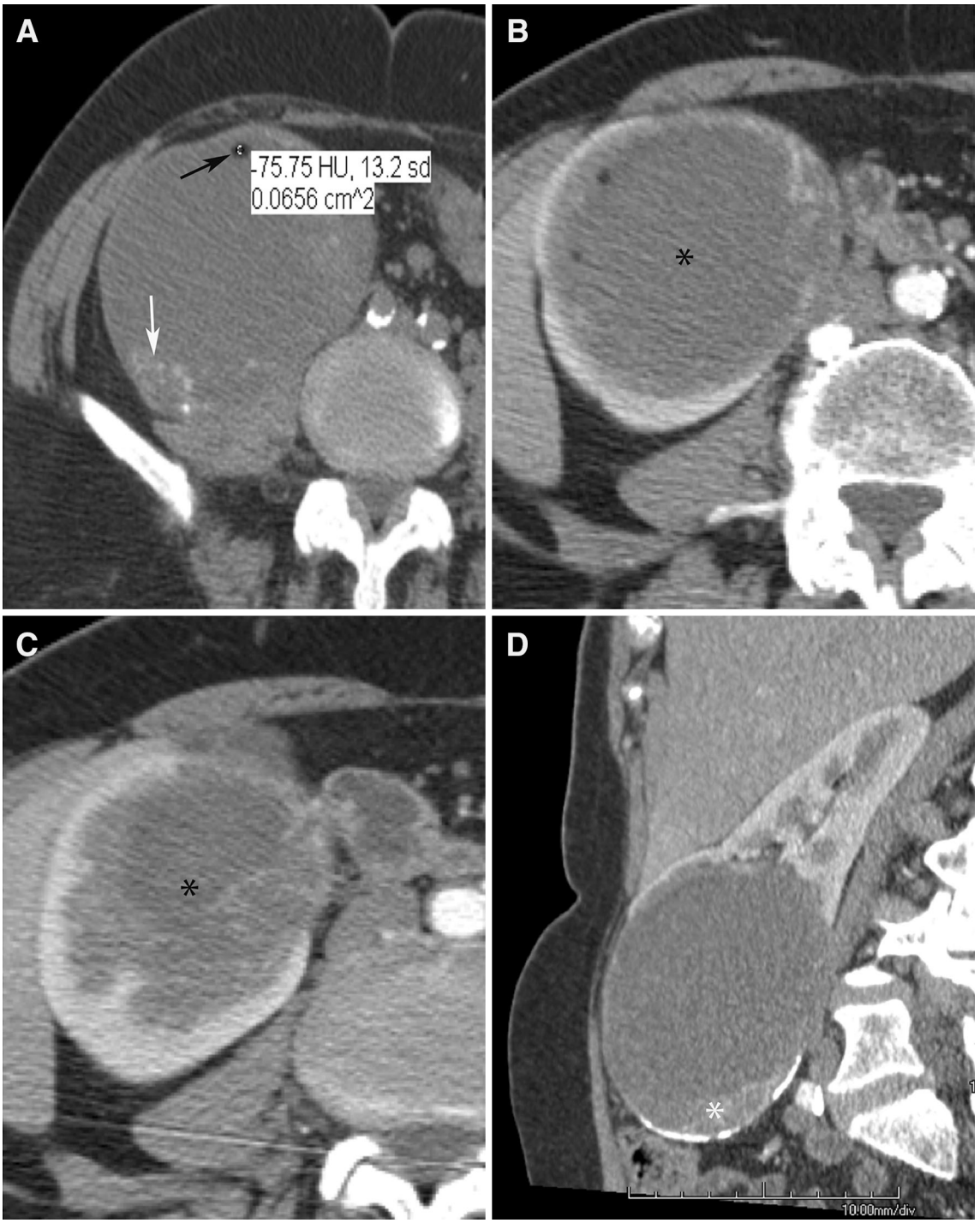

Fig. 10. Papillary RCC. **A** Axial non-contrast shows renal mass with calcifications (white arrow) and macroscopic fat (black arrow); **B**, **C** axial CECT demonstrating hypoenhancing mass (black asterisks); **D** coronal CECT shows cystic mass with solid components (white asterisk).

Fig. 11. Chromophobe RCC. **A** Axial CT pre-contrast and **B** post-contrast demonstrate a well-circumscribed renal lesion with central scar (white arrow), which is seen in approximately 40% of cases.

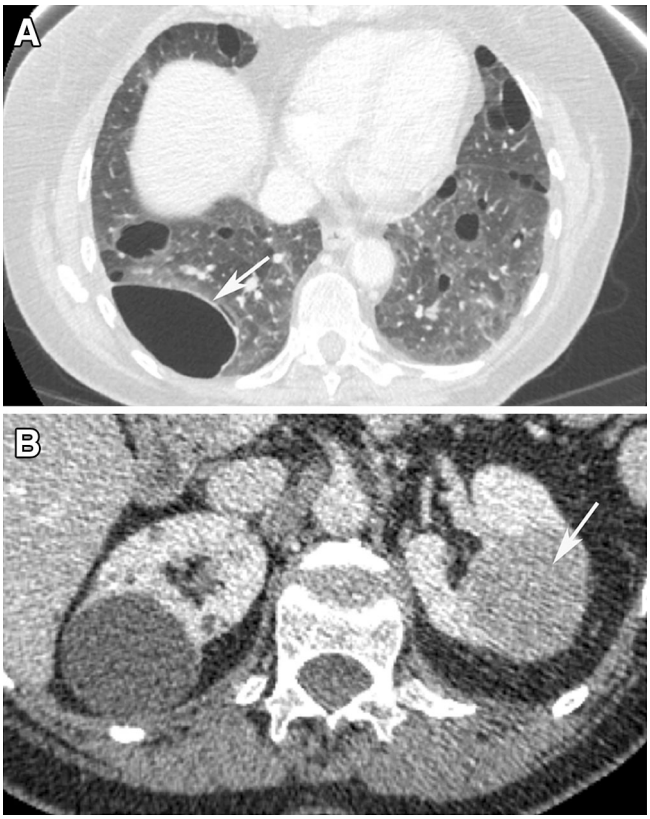

Fig. 12. Birt–Hogg–Dube syndrome. **A** Axial CECT through the chest shows multiple pulmonary cysts (white arrow). **B** Axial CECT of the abdomen demonstrates mass with the left kidney (white arrow) with less enhancement than cortex, related to chromophobe RCC.

single nodules or wedge-shaped areas that enhance less than normal parenchyma (Fig. 24) [64, 65].

Metastases

Metastatic disease to the kidney occurs in about 10% of extrarenal malignancy cases, and typically presents in the late stages of the primary disease, often with widespread metastatic disease [66, 67]. Primary neoplasms that involve the kidney more commonly are bronchogenic carcinomas, gastrointestinal adenocarcinomas, and breast malignancies. On imaging these masses are often small, multifocal and/or bilateral, and they can have an infiltrative or exophytic growth pattern, necrosis, hemorrhage, or calcifications depending on the type of primary malignancy (Fig. 25) [68].

Fig. 13. RCC XP11.2 Translocation. **A** Axial unenhanced CT shows hyperdense kidney lesion (white arrow); **B** axial delayed CECT shows capsule sign (white arrows); **C** axial T2W MR shows heterogeneity with low signal areas (white arrow).

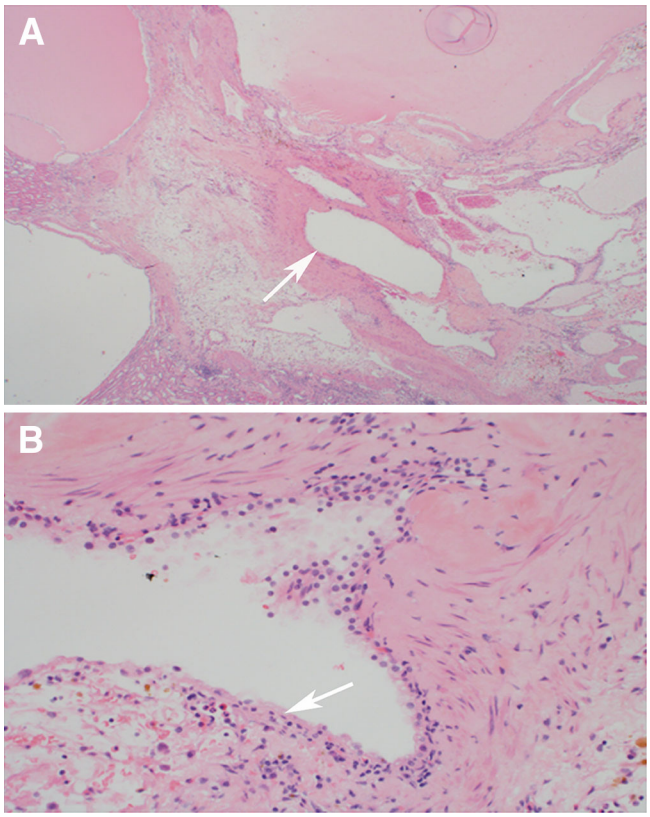

Fig. 14. Multilocular cystic RCC. **A** Photomicrograph (original magnification, × 20; hematoxylin–eosin stain) demonstrates cystic areas (white arrow); **B** photomicrograph (original magnification, × 200; hematoxylin–eosin stain) with these cystic areas lined by clear cells (white arrow). No solid nodules.

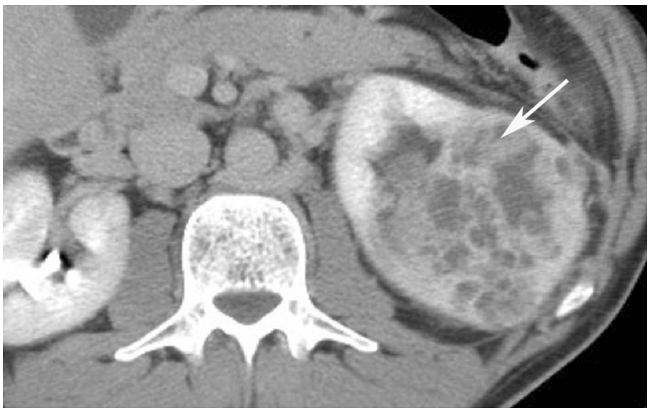

Fig. 15. Collecting duct carcinoma: CECT axial reformatted image shows large and heterogeneous mass on the left kidney, involving the renal pelvis (white arrow), and infiltrating throughout the kidney.

Conclusion

Common renal tumors may have atypical presentations and rare malignant tumors often can have characteristic appearances. Recognizing these key features can aid the radiologist in making a primary diagnosis, or troubleshoot in situations where there is a diagnostic dilemma, particularly when tissue cannot be obtained. Nevertheless, despite advances in the imaging characterizations of these lesions, pathology remains the gold standard in diagnosis.

Fig. 16. Sickle cell trait patient with medullary carcinoma. **A** Axial and **B** coronal contrast-enhanced CT images show infiltrative and hypovascular mass. Note the medullary epicenter (white arrow).

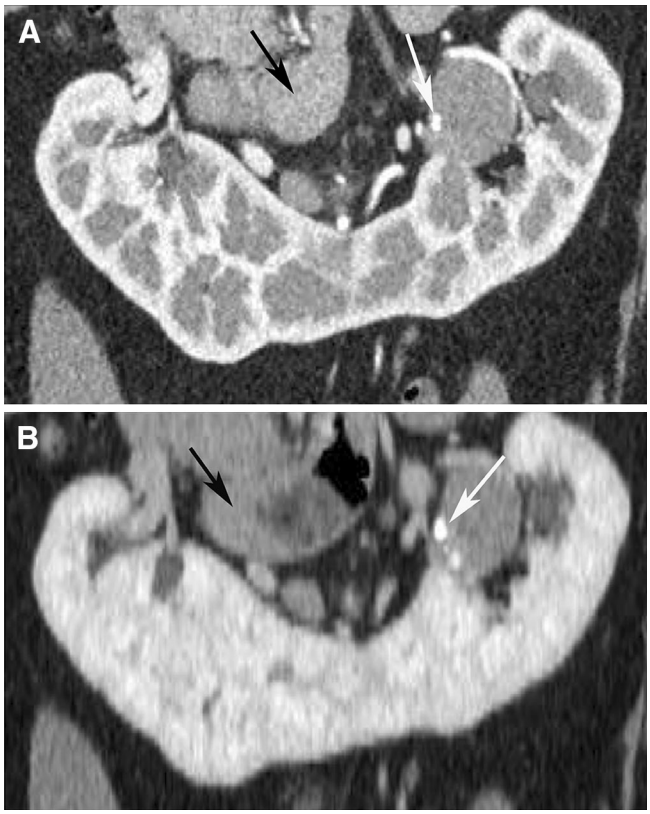

Fig. 17. Carcinoid tumor **A**, **B** curved reformatted contrast-enhanced CT show poorly enhancing mass with calcification (white arrow) within a horseshoe kidney and associated retroperitoneal lymphadenopathy (black arrow).

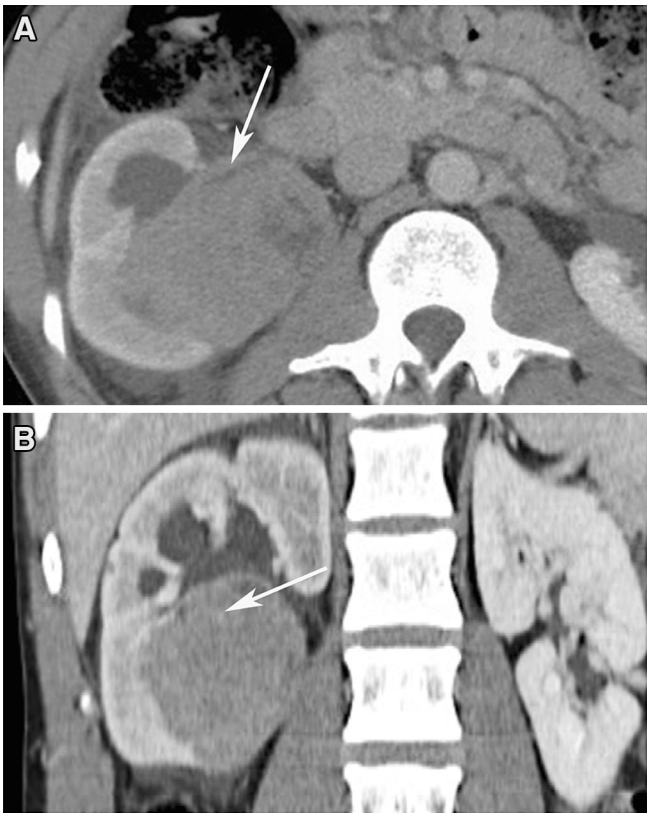

Fig. 18. Neuroendocrine carcinoma. **A** Axial CECT and **B** coronal CECT show large renal mass with medullary location (white arrows), low enhancement, and lack of necrosis.

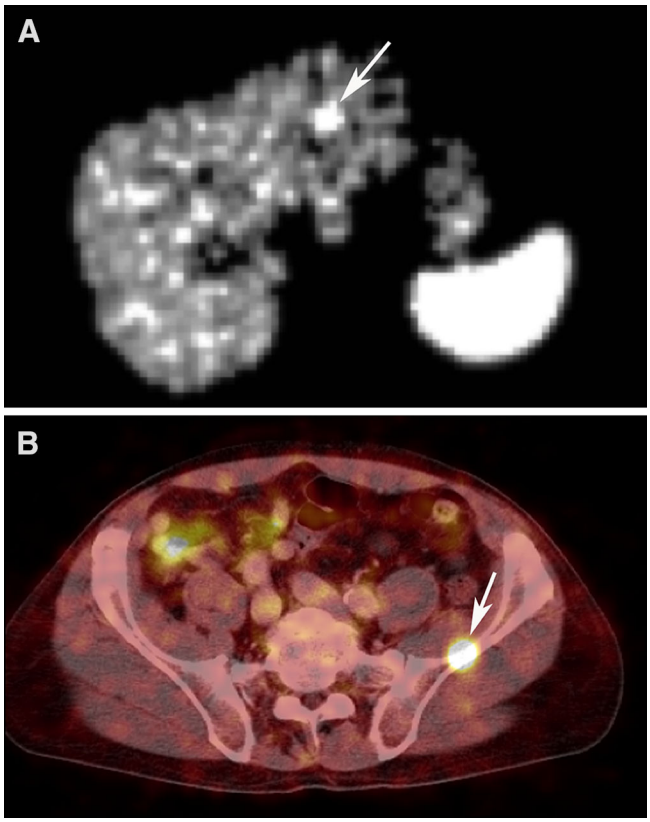

Fig. 19. **A**, **B** Octreoscan of the carcinoid case (Fig. 17). Increased radiotracer uptake in the liver and left iliac bone (white arrows), consistent with metastatic disease.

Fig. 20. Nephroblastomatosis: axial CECT shows poorly enhancing nodules (white arrows), with low-level enhancement.

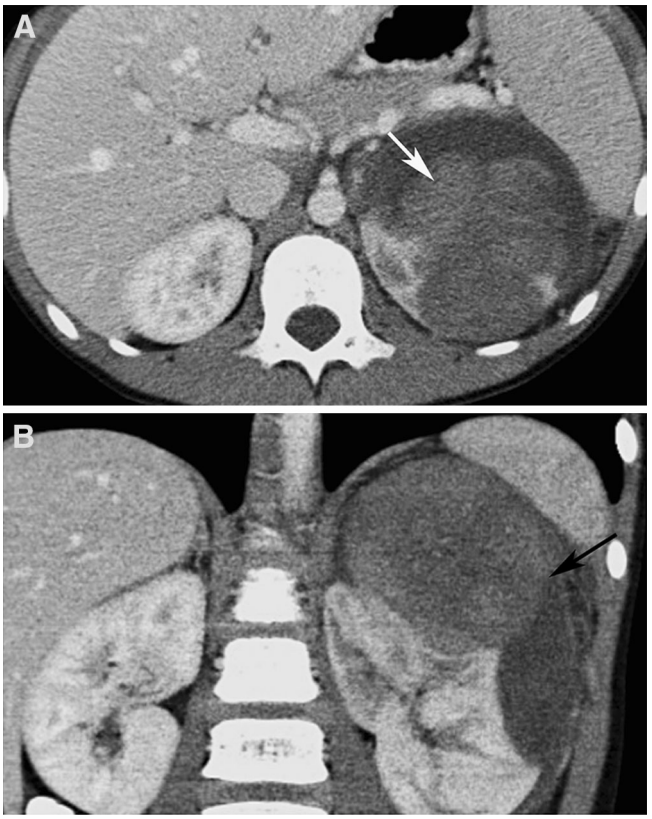

Fig. 21. Wilm's tumor. **A** Coronal and **B** axial CECT show macrolobulated mass on the left kidney (white arrow) associated with subcapsular hematoma (black arrow).

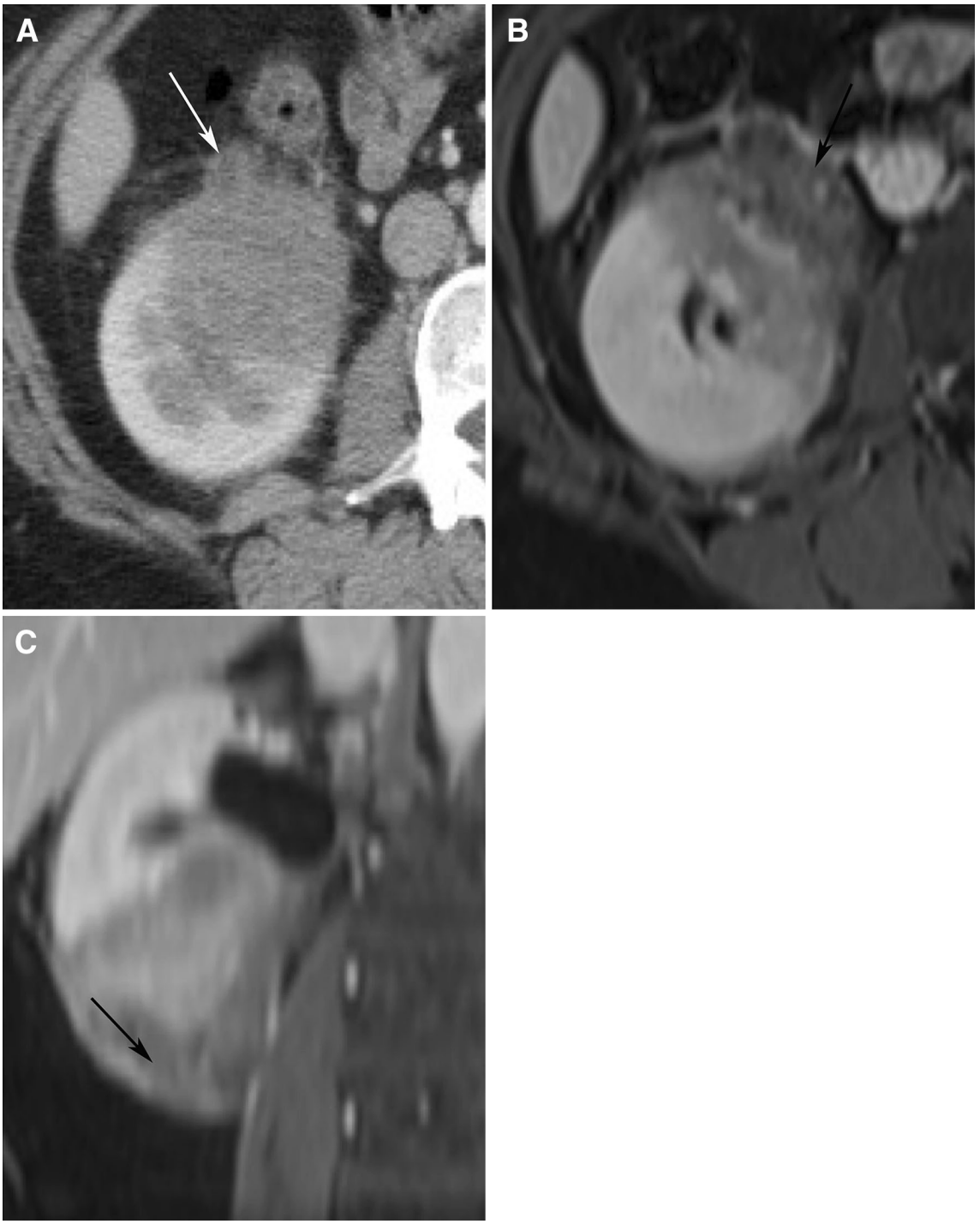

Fig. 22. Renal lymphoma. **A** Axial CECT shows solitary kidney mass with extension to perirenal fat (white arrow); **B** Axial and **C** coronal post-contrast T1W images show solitary mass on the lower pole of the right kidney (black arrows).

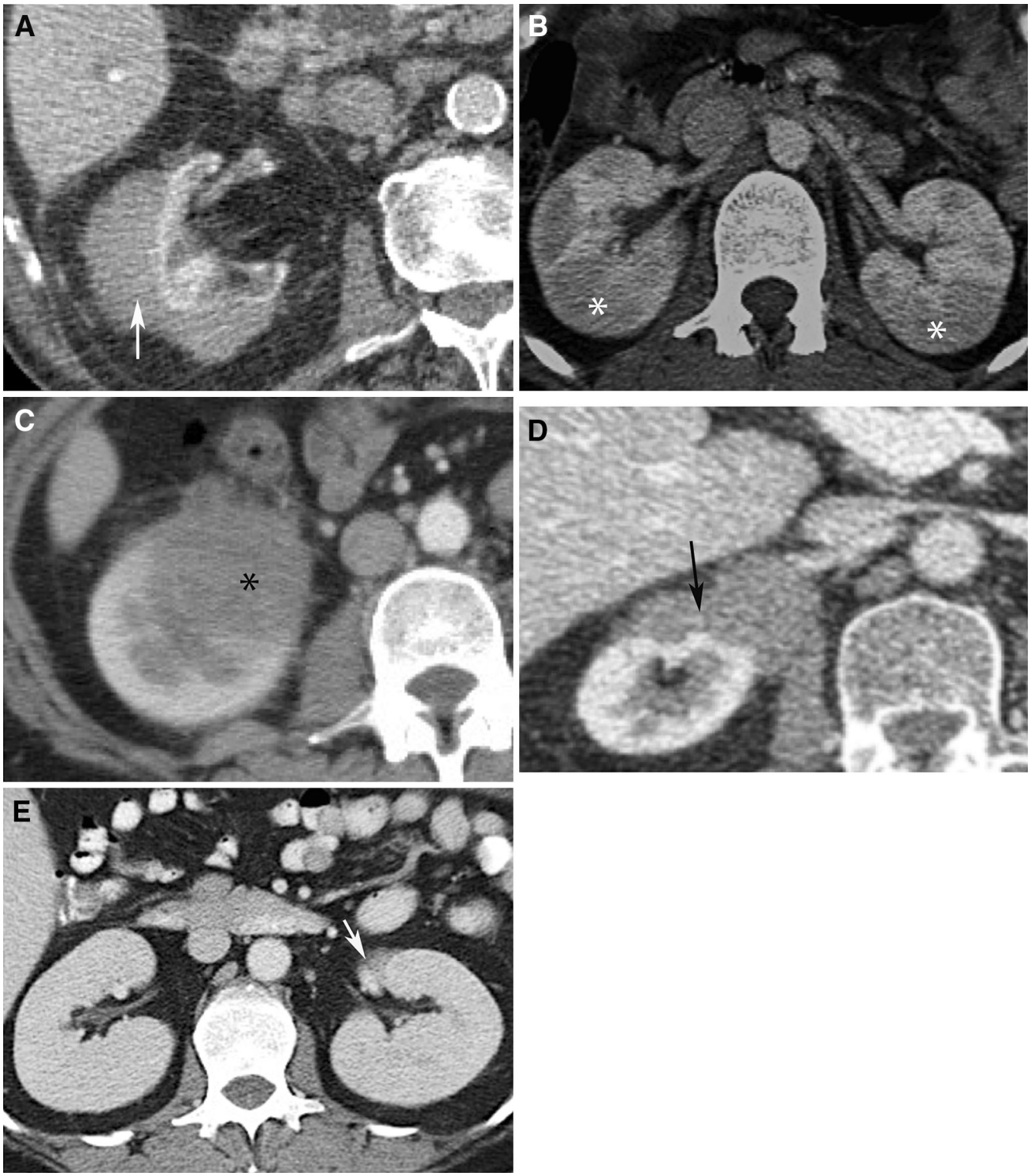

Fig. 23. Different manifestations of renal lymphoma: **A** perirenal mass (white arrow), **B** multiple masses (white asterisks), **C** solitary mass (black asterisk), **D** diffuse infiltration with nephromegaly (black arrow), and **E** invasion from retroperitoneal mass (white arrow).

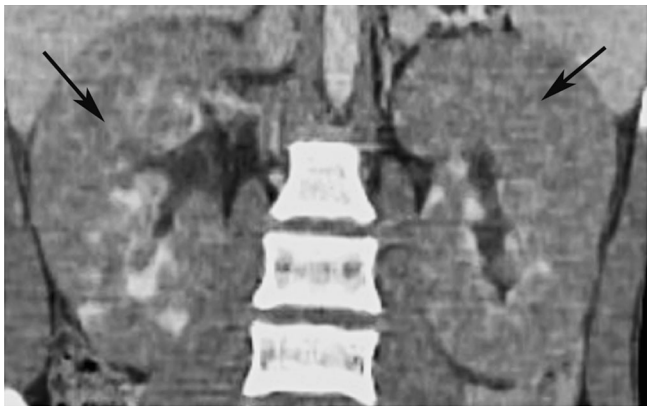

Fig. 24. Renal involvement of leukemia: coronal CECT shows nodular infiltration of both kidneys (black arrows) that enhance less than the normal parenchyma.

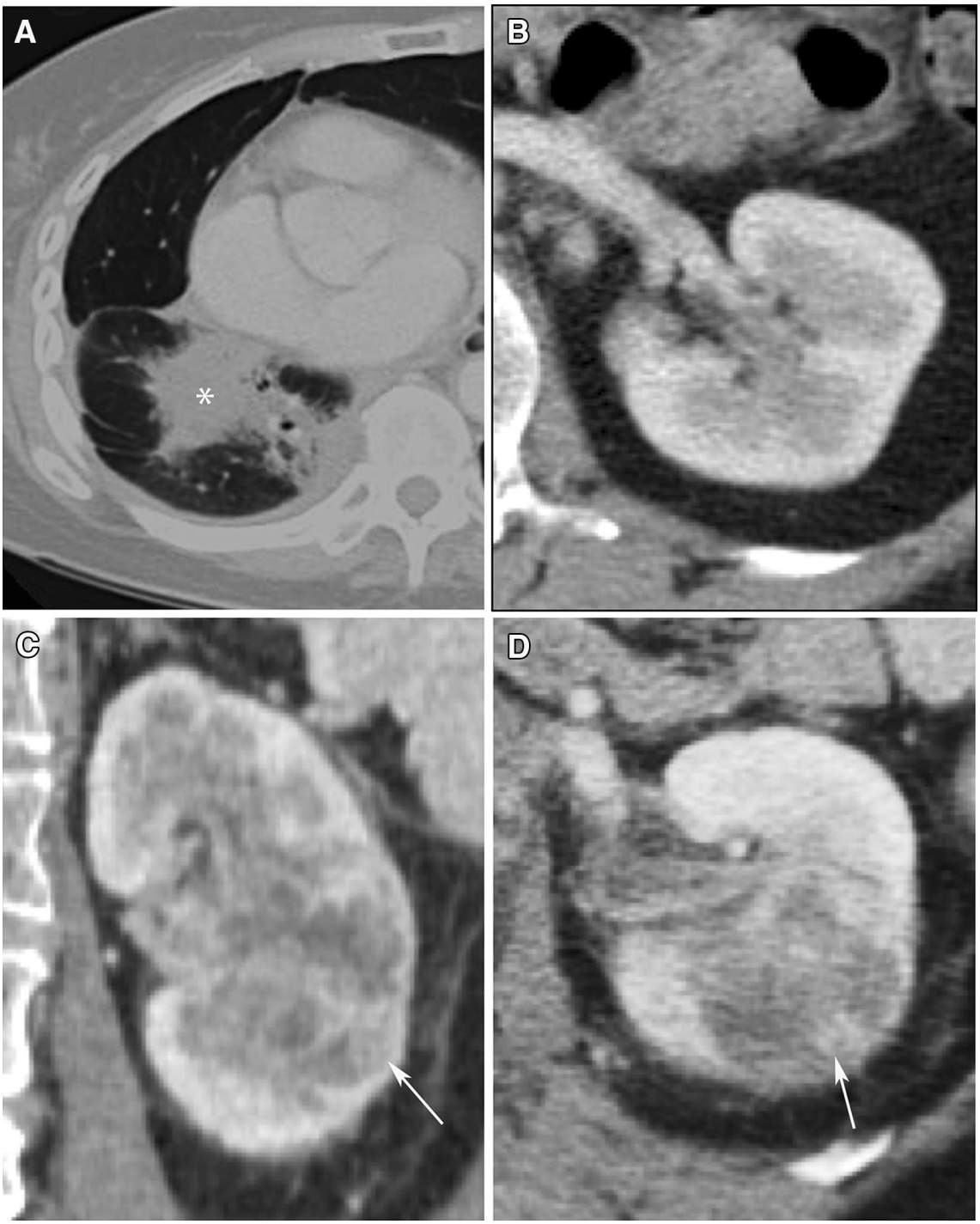

Fig. 25. Lung adenocarcinoma. **A**, **B** Axial CECT show mass (white asterisk) on the right lung and no lesion on the left kidney; **C** coronal and **D** axial CECT 6 months later show new lesion within the left kidney, with infiltrative pattern, related to metastatic disease (white arrows).

Compliance with ethical standards

Funding No funding was obtained for this paper.

Conflict of interest Antonio C. Westphalen is a scientific advisory board member for 3D Biopsy, LLC. Ronald Zagoria is a consultant for ReCor Medical, Inc. Benjamin Laguna, CT Guimarães, Zhen Whang, and Jeff Simko declare no conflicts of interest.

Ethical approval This article does not contain any studies with human participants or animals performed by any of the authors.

References

1. Pedrosa I, Sun MR, Spencer M, et al. (2008) MR imaging of renal masses: correlation with findings at surgery and pathologic analy-

sis. Radiographics 28:985–1003. https://doi.org/10.1148/rg.284065018
2. Delahunt B, Srigley JR, Delahunt B, et al. (2013) CHAPTER 1 tumours of the kidney WHO histological classification of tumours of the kidney. Int Classif 32:1469–1489. https://doi.org/10.1053/j.semdp.2015.02.002
3. Young JR, Margolis D, Sauk S, et al. (2013) Clear cell renal cell carcinoma: discrimination from other renal cell carcinoma subtypes and oncocytoma at multiphasic multidetector CT. Radiology 267:444–453. https://doi.org/10.1148/radiol.13112617
4. Kim JK, Kim TK, Kim CS, Kim K, Cho K (2002) Differentiation of subtypes of renal cell carcinoma on helical CT scans. Am J Roentgenol 178:1499–1506
5. Kang SK, Huang WC, Pandharipande PV, Chandarana H (2014) Solid renal masses: what the numbers tell us. Am J Roentgenol 202:1196–1206. https://doi.org/10.2214/AJR.14.12502
6. Sheth S, Scatarige JC, Horton KM, Corl FM, Fishman EK (2001) Current concepts in the diagnosis and management of renal cell carcinoma: role of multidetector CT and three-dimensional CT. Radiographics 21:S237–S254. https://doi.org/10.1148/radiographics.21.suppl_1.g01oc18s237
7. Oliva MR, Glickman JN, Zou KH, et al. (2009) Renal cell carcinoma: T1 and T2 signal intensity characteristics of papillary and clear cell types correlated with pathology. Am J Roentgenol 192:1524–1530. https://doi.org/10.2214/AJR.08.1727
8. Young JR, Coy H, Kim HJ, et al. (2017) Performance of relative enhancement on multiphasic MRI for the Differentiation of Clear Cell Renal Cell Carcinoma (RCC) from Papillary and Chromophobe RCC subtypes and oncocytoma. Am J Roentgenol 208:812–819. https://doi.org/10.2214/AJR.16.17152
9. Lee-Felker SA, Felker ER, Tan N, et al. (2014) Qualitative and quantitative MDCT features for differentiating clear cell renal cell carcinoma from other solid renal cortical masses. Am J Roentgenol 203:W516–W524. https://doi.org/10.2214/AJR.14.12460
10. Kang SK, Zhang A, Pandharipande PV, et al. (2015) DWI for renal mass characterization: systematic review and meta-analysis of diagnostic test performance. Am J Roentgenol 205:317–324. https://doi.org/10.2214/AJR.14.13930
11. Hotker AM, Mazaheri Y, Wibmer A, et al. (2016) Use of DWI in the differentiation of renal cortical tumors. Am J Roentgenol 206:100–105. https://doi.org/10.2214/AJR.14.13923
12. Clark PE (2009) The role of VHL in clear-cell renal cell carcinoma and its relation to targeted therapy. Kidney Int. 76:939–945
13. Karlo CA, Luigi P, Paolo D, Chaim J, Hakimi AA (2014) Radiogenomics of clear-cell renal cell carcinoma: associations between CT imaging features and mutations. Radiology 270:464–471. https://doi.org/10.1148/radiol.13130663.Radiogenomics
14. Choyke PL, Glenn GM, Walther MM, et al. (1992) The natural history of renal lesions in von Hippel–Lindau disease: a serial CT study in 28 patients. Am J Roentgenol . https://doi.org/10.2214/ajr.159.6.1442389
15. Hes FJ, Feldberg MA (1999) Von Hippel–Lindau disease: strategies in early detection (renal-, adrenal-, pancreatic masses). Eur Radiol . https://doi.org/10.1007/s003300050717
16. Ng CS, Wood CG, Silverman PM, et al. (2008) Renal cell carcinoma: diagnosis, staging, and surveillance. Am J Roentgenol 191:1220–1232. https://doi.org/10.2214/AJR.07.3568
17. Zagoria RJ, Dyer RB, Assimos DG, Scharling ES, Quinn SF (1991) Spontaneous perinephric hemorrhage: imaging and management. J Urol 145:468–471
18. Childs DD, Clingan MJ, Zagoria RJ, et al. (2014) In-phase signal intensity loss in solid renal masses on dual-echo gradient-echo MRI: association with malignancy and pathologic classification. Am J Roentgenol 203:W421–W428. https://doi.org/10.2214/AJR.13.11113
19. Taouli B, Thakur RK, Mannelli L, et al. (2009) Renal lesions: characterization with diffusion-weighted imaging versus contrast-enhanced MR imaging. Radiology 251:398–407. https://doi.org/10.1148/radiol.2512080880
20. Vikram R, Ng CS, Tamboli P, et al. (2009) Papillary renal cell carcinoma: radiologic-pathologic correlation and spectrum of disease. Radiographics 29:741–747. https://doi.org/10.1148/rg.293085190
21. Fondriest SA, Gowdy JM, Goyal M, Sheridan KC, Wasdahl DA (2015) Concurrent renal-cell carcinoma and cutaneous leiomyomas: a case of HLRCC. Radiol Case Rep 10:962. https://doi.org/10.2484/rcr.v10i1.962
22. PDQ Cancer Genetics Editorial Board (2002) Genetics of Kidney Cancer (Renal Cell Cancer) (PDQ®): Health Professional Version
23. Prasad SR, Dalrymple NC, Surabhi VR (2008) Cross-sectional imaging evaluation of renal masses. Radiol Clin N Am 46:95–111
24. Prasad SR, Humphrey PA, Catena JR, et al. (2006) Common and uncommon histologic subtypes of renal cell carcinoma: imaging spectrum with pathologic correlation. RadioGraphics 26:1795–1806. https://doi.org/10.1148/rg.266065010
25. Raman SP, Johnson PT, Allaf ME, Netto G, Fishman EK (2013) Chromophobe renal cell carcinoma: multiphase MDCT enhancement patterns and morphologic features. Am J Roentgenol 201:1268–1276. https://doi.org/10.2214/AJR.13.10813
26. Rosenkrantz AB, Hindman N, Fitzgerald EF, et al. (2010) MRI features of renal oncocytoma and chromophobe renal cell carcinoma. Am J Roentgenol . https://doi.org/10.2214/AJR.10.4718
27. Paner GP, Amin MB, Alvarado-Cabrero I, et al. (2010) A novel tumor grading scheme for chromophobe renal cell carcinoma. Am J Surg Pathol 34:1233–1240. https://doi.org/10.1097/PAS.0b013e3181e96f2a
28. Kim JI, Cho JY, Moon KC, Lee HJ, Kim SH (2009) Segmental enhancement inversion at biphasic multidetector CT: characteristic finding of small renal oncocytoma. Radiology 252:441–448. https://doi.org/10.1148/radiol.2522081180
29. Welsch MJ, Krunic A, Medenica MM (2005) Birt–Hogg–Dube syndrome. Int J Dermatol 44:668–673. https://doi.org/10.1111/j.1365-4632.2004.02095.x
30. Armah HB, Parwani AV (2010) Xp11.2 translocation renal cell carcinoma. Arch Pathol Lab Med 134:124–129. https://doi.org/10.1043/2008-0391-RSR.1
31. Chen X, Zhu Q, Li B, et al. (2016) Renal cell carcinoma associated with Xp11.2 translocation/TFE gene fusion: imaging findings in 21 patients. Eur Radiol . https://doi.org/10.1007/s00330-016-4421-4
32. Weleber RG, Watzke RC, Shults WT, et al. (2005) Clinical and electrophysiologic characterization of paraneoplastic and autoimmune retinopathies associated with antienolase antibodies. Am J Ophthalmol 139:780–794. https://doi.org/10.1016/j.ajo.2004.12.104
33. Klatte T, Streubel B, Wrba F, et al. (2012) Renal cell carcinoma associated with transcription factor E3 expression and Xp11.2 translocation: incidence, characteristics, and prognosis. Am J Clin Pathol 137:761–768. https://doi.org/10.1309/AJCPQ6LLFMC4OXGC
34. Woo S, Kim SY, Lee MS, et al. (2015) MDCT findings of renal cell carcinoma associated with Xp11.2 translocation and TFE3 gene fusion and papillary renal cell carcinoma. Am J Roentgenol 204:542–549. https://doi.org/10.2214/AJR.14.12950
35. Suzigan S, López-Beltrán A, Montironi R, et al. (2006) Multilocular cystic renal cell carcinoma: a report of 45 cases of a kidney tumor of low malignant potential. Am J Clin Pathol 125:217–222. https://doi.org/10.1309/AH6FC77PYR2V6YAY
36. Hindman NM, Bosniak MA, Rosenkrantz AB, Lee-Felker S, Melamed J (2012) Multilocular cystic renal cell carcinoma: comparison of imaging and pathologic findings. Am J Roentgenol 198:20–26. https://doi.org/10.2214/AJR.11.6762
37. Li T, Chen J, Jiang Y, et al. (2016) Multilocular cystic renal cell neoplasm of low malignant potential: a series of 76 cases. Clin Genitourin Cancer 14:e553–e557. https://doi.org/10.1016/j.clgc.2016.03.017
38. Freire M, Remer EM (2009) Clinical and radiologic features of cystic renal masses. Am J Roentgenol 192:1367–1372. https://doi.org/10.2214/AJR.08.1468
39. Kwon KA, Oh SY, Kim HY, et al. (2014) Clinical features and treatment of collecting duct carcinoma of the kidney from the korean cancer study group genitourinary and gynecology cancer committee. Cancer Res Treat 46:141–147. https://doi.org/10.4143/crt.2014.46.2.141
40. Dason S, Allard C, Sheridan-Jonah A, et al. (2013) Management of renal collecting duct carcinoma: a systematic review and the McMaster experience. Curr Oncol . https://doi.org/10.3747/co.20.1230

41. Ciszewski S, Jakimów A, Smolska-ciszewska B (2015) Collecting (Bellini) duct carcinoma : a clinical study of a rare tumour and review of the literature. Can Urol Assoc J . https://doi.org/10.3892/etm.2016.3402
42. Kuroda N, Toi M, Hiroi M, Enzan H (2002) Review of collecting duct carcinoma with focus on clinical and pathobiological aspects. Histol Histopathol 17:1329–1334
43. Hu Y, Lu G-M, Li K, Zhang L-J, Zhu H (2014) Collecting duct carcinoma of the kidney: imaging observations of a rare tumor. Oncol Lett 7:519–524. https://doi.org/10.3892/ol.2013.1739
44. Pickhardt PJ, Siegel CL, McLarney JK (2001) Collecting duct carcinoma of the kidney: are imaging findings suggestive of the diagnosis? Am J Roentgenol 176:627–633. https://doi.org/10.2214/ajr.176.3.1760627
45. Yoon SK, Nam KJ, Rha S-H, et al. (2006) Collecting duct carcinoma of the kidney: CT and pathologic correlation. Eur J Radiol 57:453–460. https://doi.org/10.1016/j.ejrad.2005.09.009
46. Baig MA, Lin Y-S, Rasheed J, Mittman N (2006) Renal medullary carcinoma. J Natl Med Assoc 98:1171–1174
47. Silvino MCM, Moniz CMV, Piotto GHM, et al. (2013) Renal medullary carcinoma response to chemotherapy: a referral center experience in Brazil. Rare Tumors . https://doi.org/10.4081/rt.2013.e44
48. Srigley JR, Delahunt B (2009) Uncommon and recently described renal carcinomas. Mod Pathol . https://doi.org/10.1038/modpathol.2009.70
49. Davidson AJ, Choyke PL, Hartman DS, Davis CJ (1995) Renal medullary carcinoma associated with sickle cell trait: radiologic findings. Radiology 195:83–85. https://doi.org/10.1148/radiology.195.1.7892499
50. Berkenblit RG, Rozenblit AM, Levin TL, et al. (2005) Renal medullary carcinoma: CT and MRI features. Am J Roentgenol 185:268–272
51. Omiyale AO, Venyo AKG (2013) Primary carcinoid tumour of the kidney: a review of the literature. Adv Urol . https://doi.org/10.1155/2013/579396
52. Degnan AJ, Tadros SS, Tocchio S (2017) Pediatric neuroendocrine carcinoid tumors: review of diagnostic imaging findings and recent advances. Am J Roentgenol 208:868–877
53. Lane B, Jour G, Zhou M (2009) Renal neuroendocrine tumors. Indian J Urol 25:155. https://doi.org/10.4103/0970-1591.52905
54. Lonergan GJ, Martínez-León MI, Agrons GA, Montemarano H, Suarez ES (1995) Nephrogenic rests, nephroblastomatosis, and associated lesions of the kidney. Radiographics 18:947–968. https://doi.org/10.1148/radiographics.18.4.9672980
55. Lowe LH, Isuani BH, Heller RM, et al. (2000) Pediatric renal masses: Wilms tumor and beyond. Radiographics 20:1585–1603. https://doi.org/10.1148/radiographics.20.6.g00nv051585
56. Sethi AT, Das Narla L, Fitch SJ, Frable WJ (2010) Best cases from the AFIP: Wilms tumor in the setting of bilateral nephroblastomatosis. Radiographics . https://doi.org/10.1148/rg.305095022
57. Samaratunga H, Delahunt B (2015) Mesenchymal tumors of adult kidney. Semin Diagn Pathol 32:160–171. https://doi.org/10.1053/j.semdp.2015.02.007
58. Katabathina VS, Vikram R, Nagar AM, et al. (2010) Mesenchymal neoplasms of the kidney in adults: imaging spectrum with radiologic–pathologic correlation. RadioGraphics 30:1525–1540. https://doi.org/10.1148/rg.306105517
59. Brisse HJ, Smets AM, Kaste SC, Owens CM (2008) Imaging in unilateral Wilms tumour. Pediatr Radiol 38:18–29
60. Sheth S, Ali S, Fishman E (2006) Imaging of renal lymphoma: patterns of disease with pathologic correlation. Radiographics 26:1151–1168. https://doi.org/10.1148/rg.264055125
61. Shetty S (2016) Primary renal lymphoma: a case report and review of literature. J Clin Diagn Res 10:9–11. https://doi.org/10.7860/JCDR/2016/20901.8577
62. Chen X, Hu D, Fang L, et al. (2016) Primary renal lymphoma: a case report and literature review. Oncol Lett 12:4001–4008. https://doi.org/10.3892/ol.2016.5173
63. Ganeshan D, Iyer R, Devine C, Bhosale P, Paulson E (2013) Imaging of primary and secondary renal lymphoma. Am J Roentgenol 201:W712–W719
64. Purysko AS, Westphalen AC, Remer EM, et al. (2016) Imaging manifestations of hematologic diseases with renal and perinephric involvement. RadioGraphics 36:1038–1054. https://doi.org/10.1148/rg.2016150213
65. Bach AG, Behrmann C, Holzhausen HJ, et al. (2012) Prevalence and patterns of renal involvement in imaging of malignant lymphoproliferative diseases. Acta Radiol 53:343–348
66. Choyke PL, White EM, Zeman RK, Jaffe MH, Clark LR (1987) Renal metastases: clinicopathologic and radiologic correlation. Radiology 162:359–363. https://doi.org/10.1148/radiology.162.2.3797648
67. Zhou C, Urbauer DL, Fellman BM, et al. (2016) Metastases to the kidney: a comprehensive analysis of 151 patients from a tertiary referral centre. BJU Int . https://doi.org/10.1111/bju.13194
68. Jain Y, Liew S, Taylor MB, Bonington SC (2011) Is dual-phase abdominal CT necessary for the optimal detection of metastases from renal cell carcinoma? Clin Radiol 66:1055–1059. https://doi.org/10.1016/j.crad.2011.06.002